Corrosion Science 71 (2013) 20–31

Contents lists available at SciVerse ScienceDirect

Corrosion Science

journal homepage: www.elsevier.com/locate/corsci

In situ inhibitor synthesis from admixture of benzaldehyde and benzene-1,2-diamine along with $FeCl_3$ catalyst as a new corrosion inhibitor for mild steel in 0.5 M sulphuric acid

Sh. Pournazari [a,*], M.H. Moayed [a], M. Rahimizadeh [b]

[a] Metallurgical and Material Engineering Department, Faculty of Engineering, Ferdowsi University of Mashhad, Mashhad 91775-1111, Iran
[b] Chemistry Department, Faculty of Science, Ferdowsi University of Mashhad, Mashhad 91775-1111, Iran

ARTICLE INFO

Article history:
Received 10 May 2012
Accepted 4 January 2013
Available online 25 January 2013

Keywords:
A. Mild steel
A. Acid solutions
B. Polarization
B. EIS
B. Weight loss
C. Acid inhibition

ABSTRACT

Corrosion protection of mild steel in 0.5 M H_2SO_4 solution was studied using combination of benzene-1,2-diamine and benzaldehyde with $FeCl_3$ to in situ synthesis of new inhibitor at different temperatures employing electrochemical, weight loss, quantum chemical studies and optical microscopy. The electrochemical results represent the combination of these components in the solution shows equal efficiency to the compound which was synthesized in the laboratory which is 2-phenyl-1H-benzo[d]imidazole. To indicate this compound was created on the metal surface, deposited layer was investigated by Fourier transform infrared spectroscopy (FTIR). Optical microscopy examinations demonstrate a decrease in corrosion attacks in presence of inhibitors.

1. Introduction

The study of mild steel and iron is a matter of tremendous theoretical and practical concern and as such has received a considerable amount of interest [1–3]. Mild steel is widely applied as constructional material in many industries due to its acceptable mechanical properties and low cost [4]. Mild steels are subjected to several industrial processes such as acid pickling, acid cleaning, acid descaling and oil well acidizing. However the main problem of applying mild steel is its dissolution in acidic solutions. Several methods are available for corrosion prevention. Employing inhibitors is one of the cost effective protection methods of metals and alloys in acids. Most of the acid corrosion inhibitors are heterocyclic organic compounds containing N, S, O and aromatic rings [5]. Study of organic corrosion inhibitors is an attractive field of research due to its usefulness in various industries [6]. It has been reported that heterocyclic organic components have better inhibition role in acidic media [7–12]. Among these, benzimidazole and its derivatives intensively were investigated as effective corrosion inhibitors in various acid solutions [13]. The organic inhibitors function through adsorption on metal surface blocking the active sites by displacing water molecules and forming a compact barrier film to decrease the corrosion rate [14]. The adsorption of inhibitors on metal / solution interface is influenced by: (i) nature and surface charge of metal; (ii) type of aggressive electrolyte; and (iii) chemical structure of inhibitors [5,13]. Benzimidazole molecule shows two anchoring sites suitable for surface bonding: the nitrogen atom with its lonely sp^2 electron pair and the aromatic rings [9,15]. So the widespread interest in benzimidazole-containing structures has prompted extensive studies for their synthesis. There are two general methods for the synthesis of 2-substituted benzimidazoles. However, all these processes require stoichiometric or excess amount of oxidants to be used. Many of these procedures produce toxic or environmentally problematic by-products often require laborious workup and purifications [16]. Thus during our research involving the application of 2-phenyl-1H-benzo[d]imidazole as a corrosion inhibitor, the combination of its components which are benzene-1,2-diamine and benzaldehyde along with ferric chloride catalyst was used as a new method of producing 2-phenyl-1H-benzo[d]imidazole in acid solution according to Fig. 1. So dc and ac electrochemical measurements including open circuit potential (OCP) as corrosion potential, linear polarization resistance (LPR) as corrosion resistance criterion, potentiodynamic polarization (PDP) and EIS tests were performed on mild steel in acid sulphuric media with different concentration of the individuals benzene-1,2-diamine and benzaldehyde as water dissolvable organic compounds and just the combination of them to study the effect of in situ synthesising of benzimidazole in acid solution in different temperatures of 25, 35, 45 and 55 °C. The 2-phenyl-1H-benzo[d]imidazole which was synthesized by the combination of these two organic compounds with catalyst in different kinds of solvents in our chemical laboratory was investigated by all the above tests to compare the inhibitive behaviour of this material

* Corresponding author. Tel.: +98 5118763305; fax: +98 5118763301.
E-mail address: sh.pournazari@gmail.com (Sh. Pournazari).

0010-938X/$ - see front matter © 2013 Elsevier Ltd. All rights reserved.
http://dx.doi.org/10.1016/j.corsci.2013.01.019

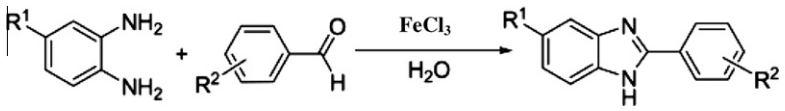

Fig. 1. Synthetic route of in situ synthesized inhibitor.

with the in situ synthesized one in the solution. In this way the material which was deposited on the steel surface was also examined by FTIR spectra. In addition to traditional techniques such as electrochemical and gravimetric measurements, quantum chemical method has been employed in this study. Invaluable quantum chemical parameters such as higher occupied molecular orbital (HOMO), lower unoccupied molecular orbital (LUMO) and dipole momentum (μ) obtained by this method, help to understand the adsorption properties by considering the structure of 2-phenyl-1H-benzo[d]imidazole which we concluded that deposited on the mild steel surface by FTIR spectra.

2. Materials and methods

In this study benzene-1,2-diamine and benzaldehyde were purchased from Merck. 2-phenyl-1H-benzo[d]imidazole was synthesized from the combination of benzene-1,2-diamine and benzaldehyde using ferric hydrogen sulphate ($Fe(HSO_4)_3$) as catalyst by Eshghi et al. [17]. Since only ferric ions were important for this reaction and ferric hydrogen sulphate was really difficult to produce, in this study ferric chloride was used instead because it is more available and cheaper. It is necessary to mention that the same procedure has been already performed by other researchers [18]. The molecular structures of the investigated compounds are given in Fig. 2. To produce in situ synthesized inhibitor, ferric chloride as catalyst was purchased from Merck. Electrolyte solution was 0.5 M H_2SO_4 and prepared from the Merck reagent sulphuric acid and double distilled water. The tests were performed on mild steel with the composition of 0.13% C; 0.51% Mn; 1.5% Cr; 0.31% Si; 0.023% P; 0.010% Al; 1.55% Ni and Fe balance all represent in weight percent (wt.%) and its preparation procedure was as follow: circular specimens with the diameter of 2.5 cm were cut from a mild steel bar stock and made by cold mounting with a self-cure epoxy resin. Before each test, specimens were ground mechanically using abrasive SiC paper of Grade Nos. 60, 120, 320, 600 and 1200 and degreased prior to washing in deionized water and dried with warm air. The tests were carried out at various temperatures (within ±1–2 °C accuracy) controlled by using a water bath. In order to reach the in situ synthesized inhibitor in the acid solution, different concentrations of benzene-1,2-diamine and benzaldehyde along with the same concentration of ferric chloride as the reactions catalyst were mixed at room temperature in 0.5 M sulphuric acid solution. The electrochemical tests have been performed using Gill AC laboratory potentiostat (ACM instrument). The used corrosion cell was standard three electrodes in which mild steel used as working electrode, the reference was the saturated calomel electrode (SCE) and a 2 cm^2 foil of platinum electrode was used as an auxiliary electrode. Before each experiment, the working electrode was immersed for 60 min in the test cell until corrosion potential reaches a steady state condition. Linear polarization resistance (LPR) was done by specimen polarization in different inhibitor concentrations from −15 to +15 mV around corrosion potential (OCP) by 10 mV/min scan rate. The R_p values have been measured by calculating the slope of the linear part of current–potential plot. Potentiodynamic polarization was conducted at constant sweep rate of 30 mV/min and scanning range of −350 to +350 mV around the open circuit potential. Electrochemical impedance spectroscopy (EIS) measurements were performed in frequency range of 30,000–0.01 Hz with amplitude of 15 mV peak-to-peak using AC signals at OCP. For the weight loss measurements mild steel coupons of dimension $2 \times 5 \times 0.37$ cm were used. Specimens were ground with silicon carbide belts 320–600 grit followed by distilled water washing then with acetone and finally dried by warm air. The weight loss was determined by weighing the cleaned samples before and after immersion in stagnant 0.5 M H_2SO_4 solution in the absence and presence of 0.0025 M in situ synthesized inhibitor which had the best inhibition efficiency for different times. In each case duplicate experiment were conducted and showed that the second result were within ±1% of the first. In order to investigate the effect of inhibitors on corrosion morphology, optical microscope has been employed. The specimen surface was mechanically polished down to 0.05 μm alumina slurry. Then, they were immersed in 0.5 M H_2SO_4 in absence and presence of 0.0001 M, 0.0005 M and 0.0025 M concentration of in situ synthesized inhibitor for 1.5 and 24 h at ambient temperature. After eliciting of each specimen from solution, it was washed and cleaned by ethanol and immediately dried with warm air. FTIR spectra were recorded in an AVATAR-370-FTIR spectrophotometer (Thermo Nicolet Company, USA). The molecular structures of benzene-1,2-diamine, benzaldehyde and 2-phenyl-1H-benzo[d]imidazole have been geometrically optimized by DFT method using B3LYP level and 3-21G** basis set with Gaussian 98. Quantum chemical parameters such as the highest occupied molecular orbital (HOMO) and the lowest unoccupied molecular orbital (LUMO) have been calculated.

3. Results

3.1. Polarization studies

Fig. 3 shows the polarization curves of mild steel in 0.5 M H_2SO_4 at 25 °C after 1 h immersion in the absence and presence of 0.0025 M benzene-1,2-diamine, benzaldehyde, combination of these two components with $FeCl_3$ which is called in situ synthesized inhibitor and the synthesized 2-phenyl-1H-benzo[d]imidazole. Similar figures were also obtained for 0.0001, 0.0005 and 0.001 which are not brought here for summary. Electrochemical parameters include corrosion potential (E_{corr}), corrosion current

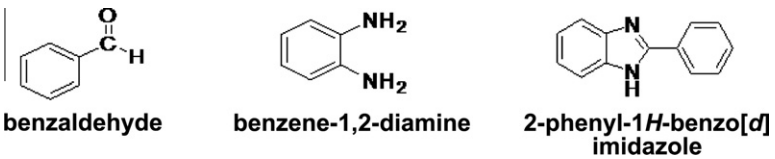

Fig. 2. Molecular structure of investigated compounds.

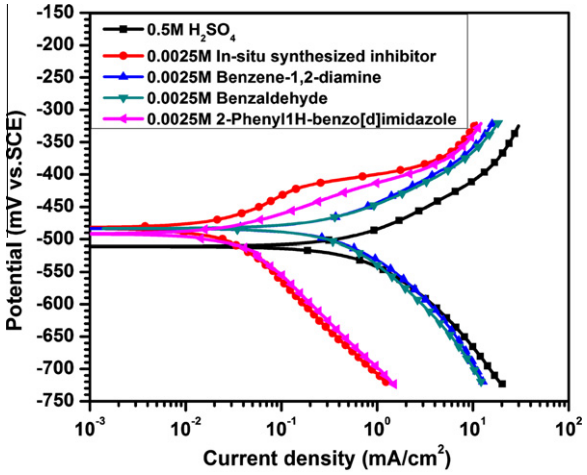

Fig. 3. Polarization curves for mild steel in 0.5 M H_2SO_4 containing 0.0025 M of the examined compounds at 25 °C.

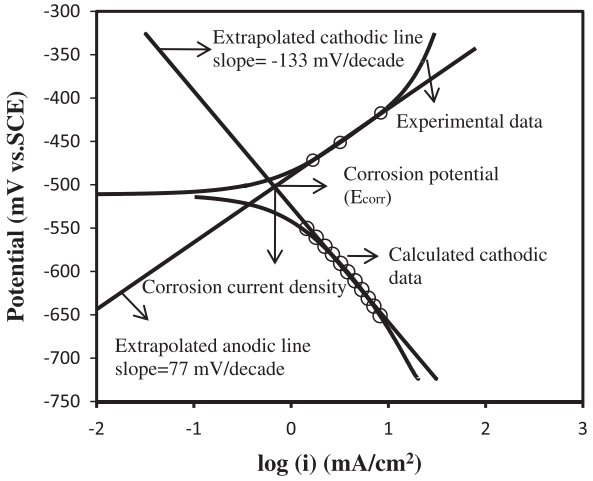

Fig. 4. Extrapolation method applied for measuring Tafel slopes, corrosion potential and corrosion current density.

density (i_{corr}) and cathodic and anodic Tafel slopes (β_c and β_a) were measured by Tafel extrapolation of the anodic and cathodic lines and listed in Table 1. The value of surface coverage (θ) was calculated using the following equation:

$$\theta = \frac{i^{\circ}_{corr} - i_{corr}}{i_{corr}} \quad (1)$$

where i°_{corr} and i_{corr} are corrosion current densities of mild steel in the absence and presence of inhibitor, respectively. Surface coverage values (θ) and the percentage of inhibition efficiency ($\%\eta = \theta \times 100$) represented in Table 1. It should be noticed that in some curves, cathodic branch does not show a complete linear Tafel behaviour, especially in the case of bulk solution. But, almost all the anodic branches show linear behaviour in one decade. To measure the cathodic Tafel slope of those curves, e.g. bulk solution cathodic Tafel slope, a method which has been previously reported by McCafferty [19] and some authors [20,21] was employed. In this way the linear part of anodic curve is extended to negative potentials (see Fig. 4) and then the cathodic current density is recalculated. Afterward, by linear extrapolating the calculated cathodic data to more positive potentials with respect to corrosion potential, the cathodic Tafel slope can be calculated. Fig. 5 represents the polarization curves of different concentrations of in situ synthesized inhibitor. The relationship between R_p (polarization resistance) and the immersion time for blank solution and 0.0025 M in situ synthesized inhibitor is shown in Fig. 6.

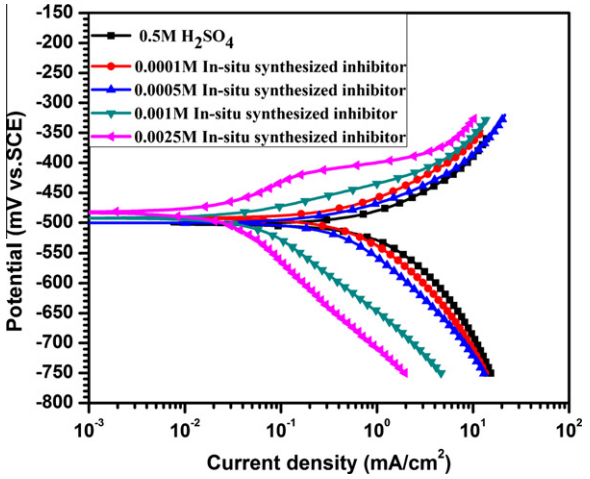

Fig. 5. Polarization curves for mild steel in 0.5 M H_2SO_4 containing different concentrations of in situ synthesized inhibitor.

3.2. Electrochemical impedance spectroscopy (EIS)

Electrochemical impedance spectroscopy (EIS) has been employed in order to investigate the surface layer created by inhibitors. The effect of inhibitor concentration on the impedance behaviour of mild steel in 0.5 M H_2SO_4 solution at 25 °C is investigated for expressed concentrations and just the results of 0.0025 M is shown in Fig. 7 for summary. Nyquist plots for mild steel at various concentrations of all compounds are nearly similar and

Table 1
Electrochemical parameters obtained from the polarization curves of different concentrations of the laboratory synthesis and in situ synthesis of 2-phenyl-1H-benzo[d]imidazole in 0.5 M H_2SO_4 solution.

Method of synthesis	Concentration	E_{corr} (mV vs. SCE)	i_{corr} (mA/cm^2)	β_a (mV/decade)	$-\beta_c$ (mV/decade)	θ	$\%\eta$
Laboratory synthesis of 2-phenyl-1H-benzo[d]imidazole	Blank	−511	0.7	77	133	–	–
	0.0001 M	−488	0.6	73	165	0.14	14
	0.0005 M	−498	0.6	77	166	0.14	14
	0.001 M	−500	0.10	63	172	0.85	85
	0.0025 M	−494	0.02	46	151	0.97	97
In situ synthesis of 2-phenyl-1H-benzo[d]imidazole	0.0001 M	−491	0.6	77	180	0.14	14
	0.0005 M	−501	0.5	81	160	0.28	28
	0.001 M	−476	0.09	46	135	0.87	87
	0.0025 M	−481	0.02	60	130	0.97	97

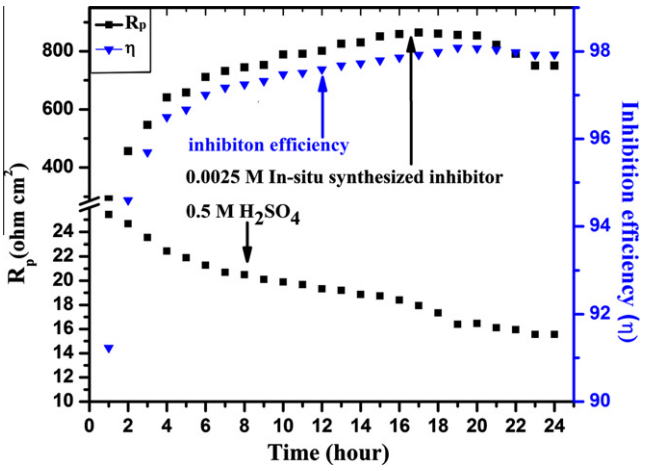

Fig. 6. Relation between R_p and immersion time and inhibition efficiency and immersion time for mild steel in 0.5 M H_2SO_4 in the presence and absence of 0.0025 M in situ synthesized inhibitor.

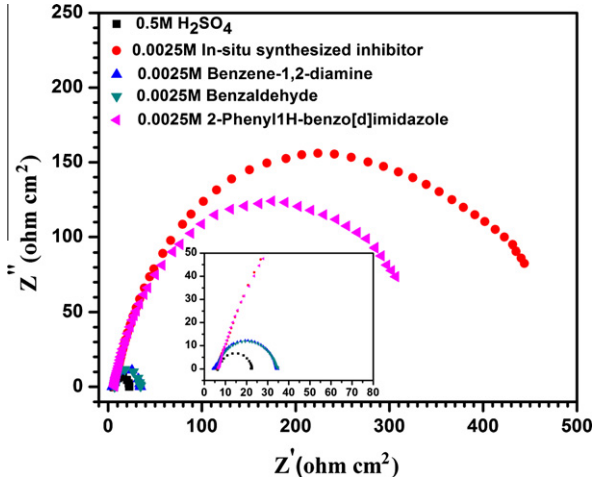

Fig. 7. Nyquist plots for mild steel in 0.5 M H_2SO_4 containing 0.0025 M of different materials at 25 °C.

contain a depressed semicircle at higher frequencies that is related to the charge transfer process. The extracted impedance parameters such as solution resistance (R_s), the charge transfer resistance (R_{ct}) and the constant phase element (CPE) parameters analyzed by EIS analyzer software from EIS plots are listed in Table 2. Inhibitor efficiency can also be estimated by charge transfer resistance according to the following equation [22]:

$$\%\eta = \frac{R - R^{\circ}}{R} \times 100 \quad (2)$$

where R° and R are charge transfer resistances of mild steel in the absence and presence of inhibitor, respectively. Calculated efficiency by charge transfer resistance is in close correlation with those obtained from polarization results. Furthermore the double layer capacitance (C_{dl}) can be calculated from the following equation [21]:

$$c_{dl} = P^{(\frac{1}{n})} R_{ct}^{(\frac{1-n}{n})} \quad (3)$$

In the above expressions P is the magnitude of CPE and n is the deviation parameter. In the Helmholtz model of the surface adsorbed film capacitance, it is defined that the capacitance is inversely proportional to the surface film thickness [23].

$$c_{dl} = \frac{\varepsilon_0 \varepsilon}{d} S \quad (4)$$

where d is the thickness of the film, S is the surface of the electrode, ε_0 is the permittivity of the air, and ε is the local dielectric constant. The decrease in C_{dl} is probably due to a decrease in local dielectric constant and/or an increase in thickness of the protective layer formed at electrode surface [21].

3.3. Linear polarization resistance

LPR method is another useful and fast method for inhibitors study. The effect of inhibitors concentration on R_p value at 25 °C has been measured and listed in Table 2. LPR results confirm the inhibitive properties of present compounds, also conclusions obtained from potentiodynamic polarization and EIS results. In addition, surface coverage and inhibitor efficiency have been calculated by Eq. (2).

3.4. Effect of temperature

The effect of temperature on the inhibited acid–metal reaction is very complex, because many changes occur on the metal surface such as rapid etching and desorption of inhibitor and the inhibitor itself may undergo decomposition [13]. The change of the corrosion rate with the temperature was studied in 0.5 M H_2SO_4, both in absence and presence of 0.0025 M of the in situ synthesized inhibitor. For this reason the polarization readings were performed at different temperatures from 25 to 55 °C in the absence and presence of different concentrations in Fig. 8. The electrochemical parameters were extracted and summarized in Table 3. As seen the inhibition efficiencies did not change considerably.

Considering the corrosion current density (i_{corr}) which corresponds to different temperatures, the activation parameter (E_a) for corrosion process can be obtained using Arrhenius equation:

$$\ln i_{corr} = \ln A - \frac{E_a}{RT} \quad (5)$$

where E_a represents the apparent activation energy, R the gas constant, A the pre-exponential factor and i_{corr} is the corrosion rate, obtained from the polarization method. Arrhenius plots for the corrosion rate of mild steel were given in Fig. 9. Values of E_a for mild steel in 0.5 M H_2SO_4 with in situ synthesized inhibitor and in the absence of inhibitor was estimated by calculating the slope of $\ln(i_{corr})$ vs. $1/T$. These results have been represented in Table 4.

3.5. Adsorption considerations

The primary step in the action of inhibitors in acid solutions is adsorption onto the metal surface, which is usually oxide-free. The existing data show that most organic inhibitors act by adsorption on the metal surface [24]. The adsorbed inhibitor then acts to retard the cathodic and/or anodic electrochemical corrosion reaction. They change the structure of the electrical double layer by adsorption on the metal surface. Basic information on the interaction between the inhibitor and the mild steel surface can be provided by the adsorption isotherm [14]. The adsorption of organic compounds can be expressed by two main types of interactions: physical adsorption and chemical adsorption [25]. Adsorption of organic molecule at the metal/solution interface can be elucidated by substitution adsorption process between the organic molecules in aqueous solution and water molecule on metal surface [6].

$$\mathrm{Org(ads)} + x\mathrm{H_2O(ads)} \rightarrow \mathrm{Org(ads)} + x\mathrm{H_2O(sol)} \quad (6)$$

where Org (sol) and Org (ads) are inhibitor molecules dissolved in solution and adsorbed on metal surface respectively. H_2O (ads) is water molecule on metal surface, H_2O (sol) is water molecule in

Table 2
Impedance parameters data and LPR results for mild steel with different concentrations of the laboratory synthesis and in situ synthesis of 2-phenyl-1H-benzo[d]imidazole in 0.5 M H_2SO_4 solution at 25 °C.

Method of synthesis	Concentration	EIS							LPR		
		R_s (Ω cm^2)	R_{ct} (Ω cm^2)	P (μF/cm^2)	n	C_{dL} (μF/cm^2)	θ	%η	R_p (Ω cm^2)	θ	%η
	Blank	6	17	365	0.86	166	–	–	24	–	–
Laboratory synthesis of 2-phenyl-1H-benzo[d]imidazole	0.0001 M	4	28	213	0.91	130	0.37	37	34	0.29	29
	0.0005 M	8	39	111	0.93	76	0.56	56	44	0.45	45
	0.001 M	7	53	131	0.88	69	0.68	68	49	0.51	51
	0.0025 M	5	611	71	0.85	41	0.97	97	397	0.94	94
In situ synthesize of 2-phenyl-1H-benzo[d]imidazole	0.0001 M	6	24	290	0.87	143	0.29	29	31	0.22	22
	0.0005 M	6	28	198	0.91	120	0.39	39	31	0.22	22
	0.001 M	5	87	155	0.90	62	0.93	93	250	0.90	90
	0.0025 M	4	500	52	0.84	27	0.96	96	440	0.94	94

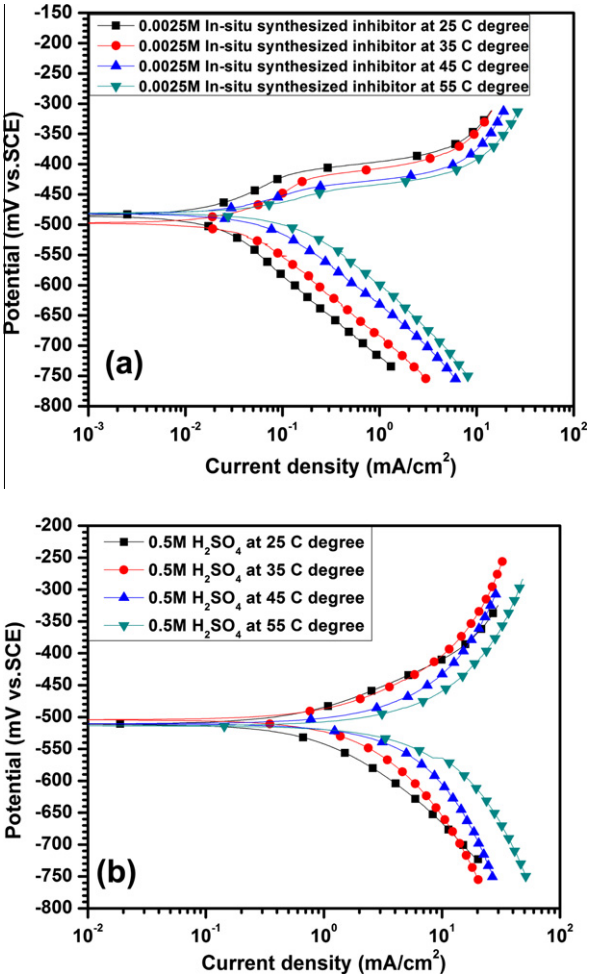

Fig. 8. Polarization curves for mild steel in different temperatures in the (a) absence of and (b) presence of 0.0025 M in situ synthesized inhibitor.

solution, and x is size ratio and represents the number of molecules of water replaced by inhibitor molecules. In order to obtain the isotherm, linear relation between θ values and inhibitor concentration C must be found. Attempts were made to fit the θ values to various isotherms including Langmuir, Temkin, Frumkin and Flory–Huggins. The Langmuir adsorption isotherm model has been used extensively in the literature for various metals, inhibitor and acid solution systems [12,26–30]. It was assumed that the adsorption of this inhibitor followed the Langmuir adsorption isotherm. According to this model the surface coverage (θ) is proportional to inhibitor concentration (C):

$$\frac{\theta}{1-\theta} = K_{ads}C \tag{7}$$

By rearranging Eq. (7):

$$\frac{C}{\theta} = \frac{1}{K_{ads}} + C \tag{8}$$

where K_{ads} is equilibrium constant for adsorption reaction. This is a general model and has been used for inhibitor studies. Fig. 10 shows the C/θ vs. C for the in situ synthesized inhibitor. According to Eq. (8), K_{ads} can be calculated from intercept line on C/θ axis. With the following equation, ΔG°_{ads} can be calculated from K_{ads}:

$$\Delta G^{\circ}_{ads} = -RT\ln(55.5K_{ads}) \tag{9}$$

where R is gas constant and T is absolute temperature of experiment and the constant value of 55.5 is the concentration of water in solution in mol dm^{-3} [4]. Normally, the magnitude of ΔG°_{ads} around −20 kJ/mol or less negative is assumed for electrostatic interactions exist between inhibitor and the charged metal surface (i.e. physisorption). Those around −40 kJ/mol or more negative are indication of charge sharing or transferring from organic species to the metal surface to form a coordinate type of metal bond (i.e. chemisorption) [11,12–18,21–32]. Some authors have reported the values of ΔG°_{ads} less negative than −40 kJ/mol for physical adsorption frequently interpreted as the formation of an adsorptive film with an electrostatic character [31,33,34]. Gibbs–Helmholtz equation can be used to calculate the heat of adsorption process (ΔH°_{ads}). With good estimation, Δc_p reaction can be considered as constant value, thus ΔH°_{ads} of reaction and Gibbs–Helmholtz equation will appear as follows [21]:

$$\Delta H^{\circ}_{ads} = \Delta c_p T + A \tag{10}$$

$$\ln K = \frac{\Delta c_p}{R}\ln T - \frac{A}{RT} + B \tag{11}$$

where A and B are equation constants and K is equilibrium constant of reaction. Using Eqs. (7), (9), and (11), the surface coverage is related to temperature:

$$\ln\left(\frac{\theta}{1-\theta}\right) = \frac{\Delta c_p}{R}\ln T - \frac{A}{RT} + B' \tag{12}$$

in which θ and B' are surface coverage and equation constant, respectively. By solving Eq. (12) for different surface coverage in presence of 0.0025 M in situ synthesized inhibitor at various temperatures (Table 3), Δc_p and A constants were obtained and according to Eq. (10), ΔH°_{ads} was calculated at 298 K and presented in Table 4. The entropy of adsorption process (ΔS°_{ads}) which is brought in Table 4 can be calculated based on the following thermodynamic basic equation [24,35]:

Table 3
Electrochemical parameters obtained from the polarization curves at different temperatures.

Examined solution	Temperature (°C)	E_{corr} (mV vs. SCE)	i_{corr} (mA/cm^2)	β_a (mV/decade)	$-\beta_c$ (mV/decade)	θ	%η
0.5 M H_2SO_4	25	−511	0.7	77	133	–	–
	35	−509	1.6	79	140	–	–
	45	−511	2.2	70	132	–	–
	55	−513	3.5	83	143	–	–
0.0025 M In situ synthesized inhibitor	25	−481	0.02	60	130	0.97	97
	35	−497	0.04	83	137	0.97	97
	45	−480	0.06	40	130	0.97	97
	55	−492	0.2	45	147	0.94	94

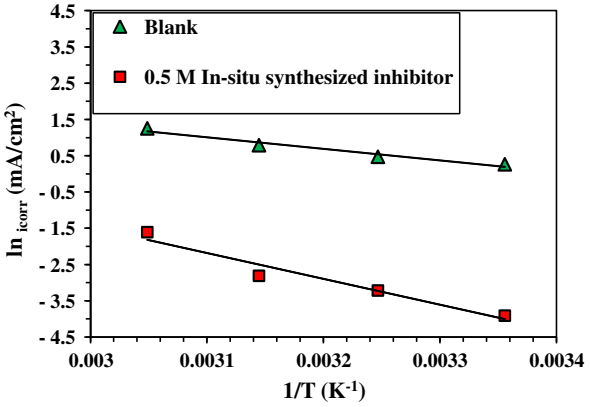

Fig. 9. ln(i_{corr}) vs. 1/T for mild steel dissolution in 0.5 M H_2SO_4 in the absence and presence of 0.0025 M in situ synthesized inhibitor.

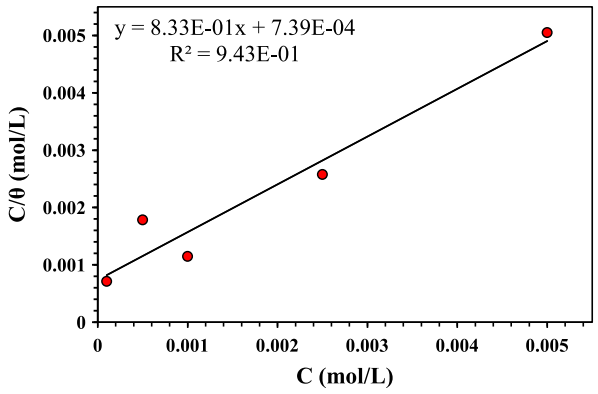

Fig. 10. Langmuir adsorption isotherm of the combination in 0.5 M H_2SO_4 at 25 °C.

Table 4
Thermodynamic parameters for adsorption of in situ synthesized inhibitor on mild steel surface in 0.5 M H_2SO_4 solution.

Examined solution	E_a (kJ/mol)	ΔG°_{ads} (kJ/mol)	ΔH°_{ads} (kJ/mol)	ΔS°_{ads} (J/mol K)
0.5 M H_2SO_4	42	–	–	–
0.0025 M In situ synthesized inhibitor	59	−27.8	−23.7	13

Table 5
Corrosion rates of mild steel in 0.5 M H_2SO_4 in the absence and presence of 0.0025 M in situ synthesized inhibitor at different times.

Examined solution	Corrosion rate (mg cm^{-2} h^{-1})			
	24 h	48 h	72 h	96 h
0.5 M H_2SO_4	0.29	0.49	0.52	0.54
0.0025 M In situ synthesized inhibitor	0.02	0.02	0.02	0.02

$$\Delta G^\circ_{ads} = \Delta H^\circ_{ads} - T\Delta S^\circ_{ads} \quad (13)$$

An endothermic adsorption process ($\Delta H^\circ_{ads} > 0$) is due to chemisorptions while an exothermic one ($\Delta H^\circ_{ads} < 0$) may be attributed to physisorption, chemisorption or a mixture of both [12,21]. In an exothermic process, physisorption can be distinguished from chemisorption by considering the absolute value of ΔH°_{ads}. For physisorption, ΔH°_{ads} is lower than 40 kJ/mol while for chemisorption, ΔH°_{ads} approaches 100 kJ/mol [4,12,22,32,36,37].

3.6. Weight loss measurements

Weight loss measurements of mild steel subjected to the effects of acidic media in the absence and presence of 0.0025 M concentration of the in situ synthesized inhibitor were made after different times of immersion at room temperature. The corrosion rates (mg cm^{-2} h^{-1}) were shown in Table 5. The inhibition efficiencies were calculated from Eq. (14) and represented in Table 6.

Table 6
Percentage inhibition efficiency of in situ synthesized inhibitor in 0.5 M H_2SO_4.

Examined solution	%Inhibition efficiency with time in hour			
	24	48	72	96
0.5 M H_2SO_4	–	–	–	–
0.0025 M In situ synthesized inhibitor	91.40	94.75	94.90	95.01

$$\%\eta = \frac{w_0 - w_i}{w_0} \times 100 \quad (14)$$

where w_0 and w_i are the values of corrosion weight loss of mild steel in uninhibited and inhibited solutions, respectively. Fig. 11 shows the plot of weight loss vs. time for mild steel in 0.5 M H_2SO_4 without and with 0.0025 M of the in situ synthesized inhibitor.

3.7. Corrosion attack morphology

Corrosion attack morphologies in absence and presence of different concentrations of in situ synthesized inhibitor after 1.5 and 24 h have been investigated by employing optical microscopy and presented in Figs. 12 and 13, respectively. In both times, it is obvious that by increasing inhibitor concentration the corrosion attack decreases. For instance the corrosion attack decrease from 0.0001 M to 0.0005 M and reaches its minimum deteriorated in the case of 0.0025 M in both times.

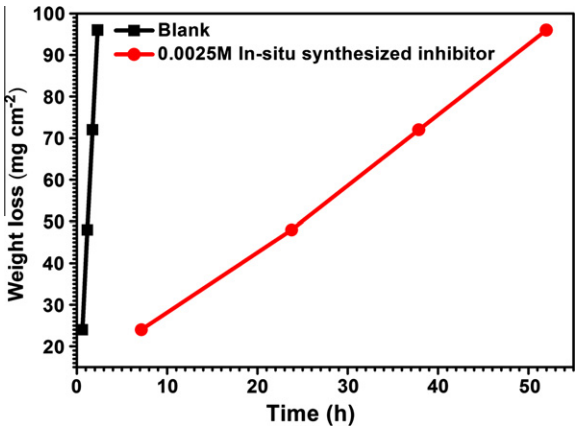

Fig. 11. Variation of weight loss against time for mild steel corrosion in 0.5 M H_2SO_4 in the presence of 0.0025 M combination.

3.8. FTIR spectra

Fourier transform infrared spectroscopy is a well-established characterization tool offering a 'fingerprint' for chemical compounds [38,39]. The FTIR reflectance spectrum of corrosion layer formed on the steel surface after immersion in 0.5 M H_2SO_4 with 0.0025 M in situ synthesized inhibitor and the 2-phenyl-1H-benzo[d]imidazole which is synthesized in the laboratory are shown in Fig. 14a. The FTIR reflectance spectrum of the commercial 2-phenyl-1H-benzo[d]imidazole is shown in Fig. 14b.

3.9. Quantum chemical calculations

Being obvious that the layer which was deposited on the metal surface was 2-phenyl-1H-benzo[d]imidazole with FTIR techniques, we investigated the correlation between molecular structure of this organic compound and its inhibition effect with quantum chemical study. So geometric structures and electronic properties of 2-phenyl-1H-benzo[d]imidazole has been calculated by DFT method using B3LYP level and 3-21G** basis set. These analysis have been employed for benzaldehyde and benzene-1,2-diamine too. Figs. 15 and 16 show optimized molecular structures, HOMO and LUMO of the studied molecules and reveal that the benzene ring and N atoms have larger electronic density. Type of benzene ring electrons is π-bonding electrons while for N atoms those are non-bonding electrons pair. It is suggested that the benzene ring and N atoms can be suitable places for adsorption onto surface, especially in the case of N atoms because of having lone pairs of electrons. Molecules of present inhibitor can be directly adsorbed at the steel surface on the basis of donor acceptor interactions between π-electrons of benzene ring, nonbonding lone pairs of N atoms, and vacant d-orbitals of iron atoms. Quantum chemical

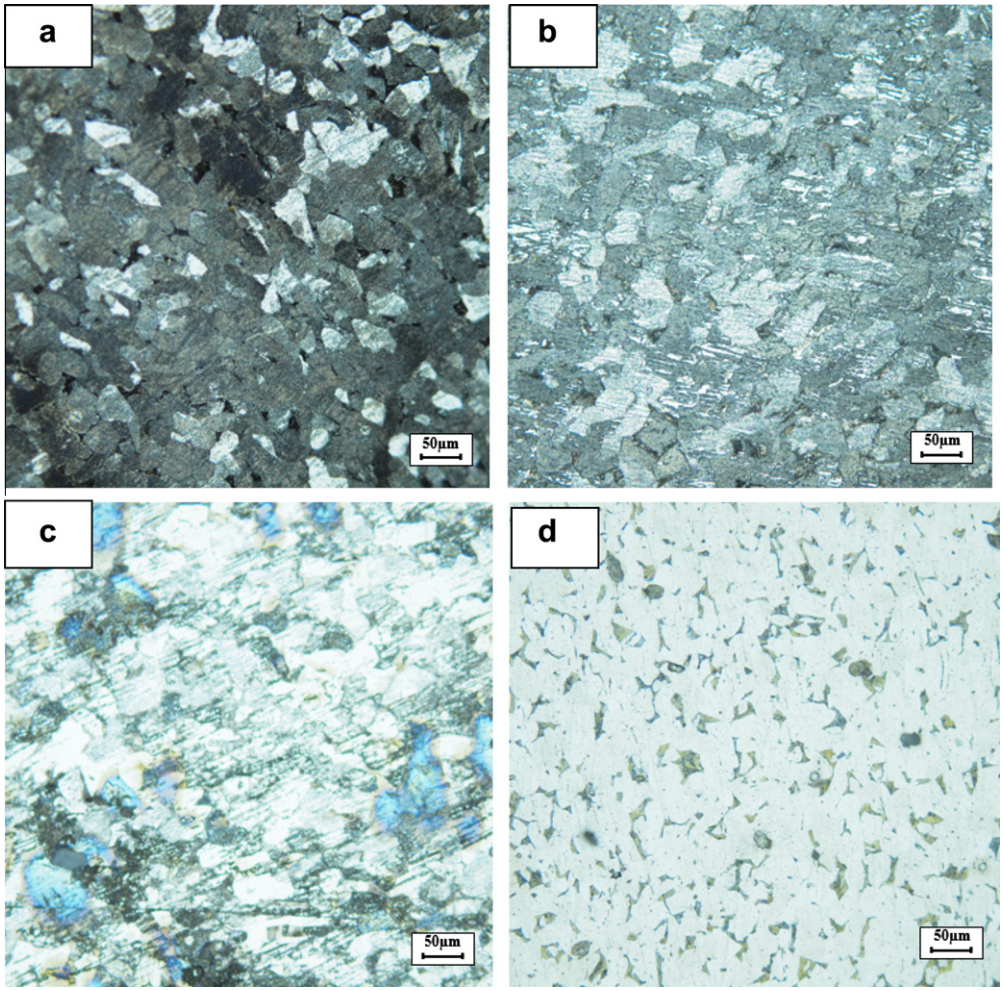

Fig. 12. Corrosion attack morphology after 1:30 h (a) blank solution (b) in the presence of 0.0001 M in situ synthesized inhibitor (c) in the presence of 0.0005 M in situ synthesized inhibitor (d) in the presence of 0.0025 M in situ synthesized inhibitor.

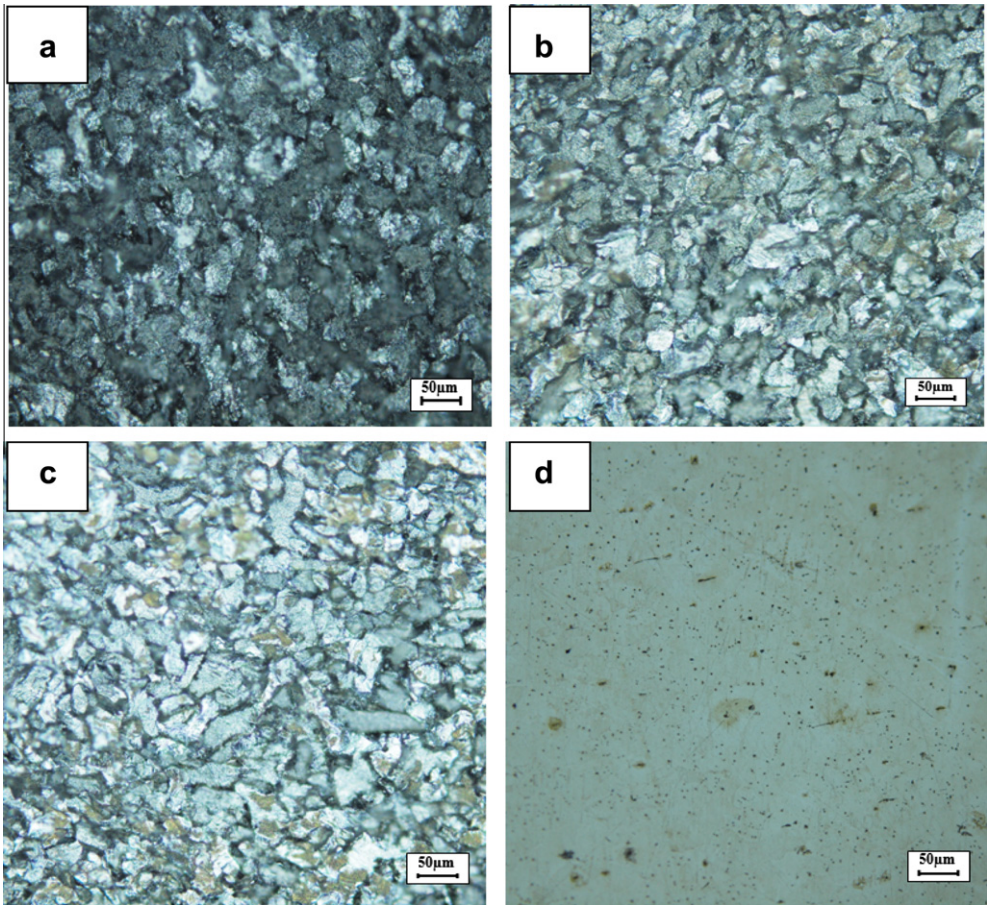

Fig. 13. Corrosion attack morphology after 24 h (a) blank solution (b) in the presence of 0.0001 M in situ synthesized inhibitor (c) in the presence of 0.0005 M in situ synthesized inhibitor (d) in the presence of 0.0025 M in situ synthesized inhibitor.

indices containing E_{HOMO}, E_{LUMO}, $\Delta E(\Delta E = E_{LUMO} - E_{HOMO})$ and Dipole moment (μ) for the studied molecules have been presented in Table 7. It has been reported that good inhibition corrosion properties are usually obtained using organic compounds that not only offer electrons to unoccupied orbitals of the metal but also accept free electrons from the metal by using their anti-bond orbitals to form stable chelates [17,18]. By looking to the Fig. 15, it is understandable that this inhibitor also could accept the d-orbital electrons of iron by LUMO on the benzene ring and N atoms. Consequently, this electron acceptance could help to form more stable bond between inhibitor molecule and iron surface.

4. Discussion

With a brief glance to Fig. 3 which indicates the polarization curves of mild steel in 0.5 M H_2SO_4 at 25 °C, it is clear that the net cathodic current densities for benzene-1,2-diamine, benzaldehyde in the 0.0025 M concentration and blank solution are similar. This is obvious for anodic part except a slight difference up to −350 mV, which means that the inhibitive properties of these organic compounds are not noticeable. It is also shown that the combination of these components by in situ inhibitor synthesis manner have the better inhibitive performance in compared with themselves individually and the equal one to the synthesized 2-phenyl-1H-benzo[d]imidazole. Therefore, using 2-phenyl-1H-benzo[d]imidazole can be replaced efficiently by using the combination of its components as a new method of in situ producing this organic compound in acid solution according to Fig. 1. Assessment of Table 1 data, it is evident that increasing concentration of the inhibitor resulted in a decrease in the corrosion current densities and an increase in%η, suggesting that the adsorption protective film tend to be more complete and stable on mild steel surface [40]. It is seen that E_{corr} shifts slightly in positive direction with concentration increase and both anodic and cathodic branches towards lower currents. Hence in situ synthesized inhibitor acts as mixed type inhibitor with predominantly control of anodic reaction [40–44]. As seen from Fig. 5 the cathodic corrosion current densities decreased dramatically, revealing that the addition of in situ synthesized inhibitor does not change the cathodic hydrogen evolution mechanism and the decrease of H^+ ions on surface of mild steel takes place mainly through a charge transfer mechanism. However in the anodic part of polarization curve of 0.0025 M inhibitor concentration, initially, the corrosion current densities increased with the potential shifting positively, which means that the adsorption process is dominant. When the polarization potential moved positively to about −400 mV, desorption of the inhibitor occurred and corrosion current densities increased markedly in compared with the initial stage. As the potential passed approximately −450 mV, the polarization behaviour resembled that in blank solution which implies that inhibitor thoroughly desorbed from the surface [34,40]. The relationship between R_p values and immersion time in Fig. 6 represented that the R_p values for mild steel in 0.5 M H_2SO_4 without inhibitor (blank) decrease with immersion time but the R_p values for mild steel in 0.5 M H_2SO_4 with the inhibitor increase with immersion time. There for the inhibition efficiency increases with the increase in the time of immersion.

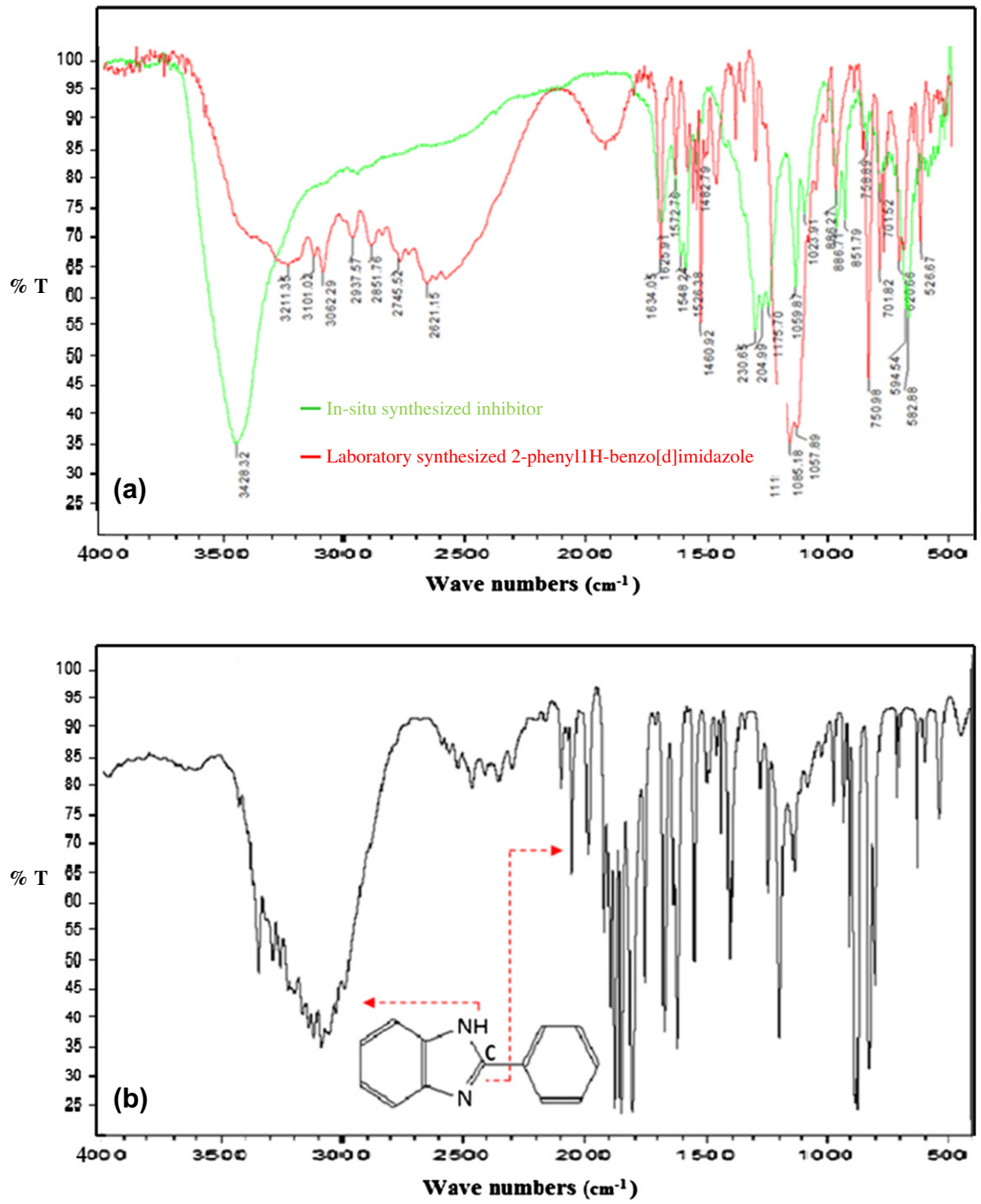

Fig. 14. (a) FTIR spectra of mild steel after immersion in 0.5 M H_2SO_4 solution with 0.0025 M in situ synthesized inhibitor and 0.0025 M laboratory synthesized 2-phenyl-1H-benzo[d]imidazole; (b) FTIR spectra for the commercial 2-phenyl-1H-benzo[d]imidazole.

The corrosion behaviour of mild steel in 0.5 M H_2SO_4 in the presence of the studied compounds investigated by EIS method at 25 °C is represented in Fig. 7 and the extracted data listed in Table 2. From Fig. 7 it is obvious that the impedance response of mild steel is significantly changed after adding in situ synthesized inhibitor in compared whit its components separately and blank solution. An increase in semi-circle diameter is indicating an increase in corrosion resistance of mild steel in presence of inhibitors. As seen from Table 2, the R_{ct} values increased with increase in inhibitor concentration. This indicates formation of an insulated adsorption layer. The values of double-layer capacitance (C_{dl}) decrease with increasing in the concentration of employed organic compounds which is due to the steady replacement of water molecules by the adsorptive inhibitor molecules at metal/solution interface, which is leading to a protective film on the steel surface and increasing the d value [4]. Although the decrease in efficiencies which were obtained from LPR method is not ignorable, these values are close to those calculated by polarization and EIS methods. The difference between obtained efficiencies from LPR and EIS results can be attributed to the fact that, in EIS results, the effect of solution resistance (R_s) is not considered. However the results of LPR method contain this parameter as well as charge transfer resistance.

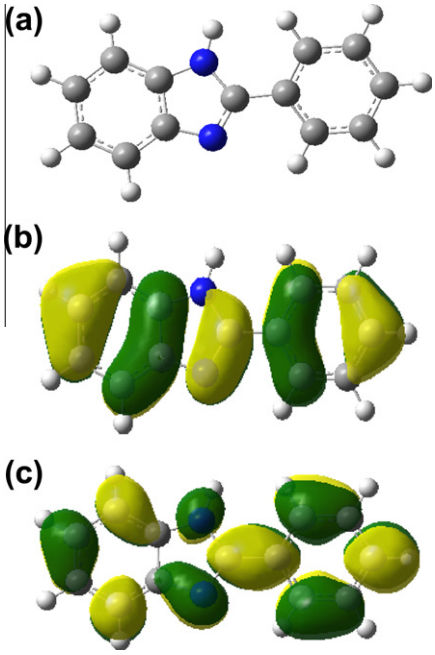

Fig. 15. (a) Molecular structure, (b) HOMO and (c) LUMO of 2-phenyl-1H-benzo[d]imidazole.

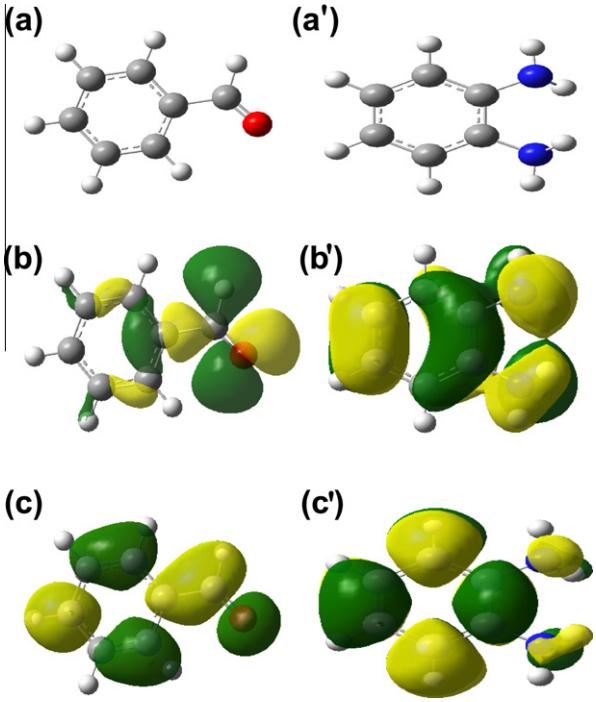

Fig. 16. (a) Molecular structure, (b) HOMO and (c) LUMO of benzaldehyde; (a′) Molecular structure (b′) HOMO and (c′) LUMO of benzene-1,2-diamine.

Table 7
HOMO and LUMO values of the studied molecules calculated by DFT method.

Quantum chemical parameters	2-Phenyl-1H-benzo[d]imidazole	Benzene-1,2-diamine	Benzaldehyde
E_{HOMO}	−5.95	−5.24	−7.15
E_{LUMO}	−1.44	0.19	−1.93
$\Delta E = E_{LUMO} - E_{HOMO}$	4.51	5.44	5.22
Dipole moment	3.13	1.38	2.99

The change of the corrosion rate with the temperature was studied in 0.5 M H_2SO_4, both in absence and presence of 0.0025 M of the in situ synthesized inhibitor and the electrochemical parameters were extracted and summarized in Table 3. Although, Table 3 data obviously shows an increase in corrosion rate with rising in temperature, however the corrosion rate of inhibited solutions is always lower than the blank one. So raising the temperature did not change the inhibition efficiencies. As it is shown from Arrhenius plots in Fig. 9 and the results in Table 4, by synthesizing inhibitor in solution containing 0.5 M H_2SO_4, the activation energy for corrosion process increases from 42 kJ/mol to 59 kJ/mol. The increase in the corrosion current density activation energy indicates that dissolution of mild steel in 0.5 M H_2SO_4 in the presence of inhibitor is lower than the solution with no inhibitor. It has been reported that higher E_a in presence of inhibitors for mild steel in comparison with blank solution is typically showing physisorption [21]. Considering E_a values, the combination has an electrostatic interaction on metal surface (physisorption).

The C/θ when plotted vs. C for the in situ synthesized inhibitor in Fig. 10 demonstrates that adsorption of this inhibitor on mild steel follow the Langmuir isotherm and supposed that the adsorbed molecules occupy only one site and there are no interactions with other adsorbed species [31]. The thermodynamic parameters calculated and listed in Table 4. As it is represented in this table ΔG°_{ads} for the in situ synthesized inhibitor will be −27.8 kJ/mol. The calculated ΔG°_{ads} value was within −40 and −20 kJ/mol. This reflects electrostatic interaction between the inhibitor and positively charged metal surface and maybe described by physical adsorption [45]. Since ΔH°_{ads} was negative, the adsorption of in situ synthesized inhibitor molecules onto the mild steel surface was an exothermic process. On the other hand, the value of ΔH°_{ads} is indicating physisorption mechanism that is in agreement with results obtained by activation parameter (E_a) [4,21]. The positive sign of ΔS°_{ads} arise from substitutional process, which can be attributed to the increase in the solvent entropy and more positive water desorption entropy [4,33,38,46].

By the weight loss measurements for inhibited solution the corrosion rates changed slightly with increasing exposure time while it was increased dramatically for blank solution. So the inhibition efficiencies were increased with increasing time and reached 95% after 96 h (Tables 5 and 6). From Fig. 11 it is very obvious that the weight loss of mild steel in the different test solutions increases with time. It is also clear that weight loss of mild steel decreases with introduction of the inhibitor into the acid solution indicating this inhibitor functioned as an inhibitor isolating the metal from attack by the aggressive anions present in the solution [22].

It can be clearly seen that in the absence of inhibitor after 1:30 h (Fig. 12a), the specimen surface has been severely corroded. At same time, the corrosion attack is significantly lower than uninhibited solution in presence of in situ synthesized inhibitor. Surface evaluation of specimen immersed during 1.5 h, reveals that mirror-like polished specimen surface has been just partially etched after immersion test, while the surface of specimen in absence of inhibitor has changed to rough and a black appearance due to severe corrosion. With comparing Figs. 12 and 13 it can be clearly seen that by increasing the time of immersion from 1.5 to 24 h the surface of specimen which was immersed in blank solution deteriorated completely while the surface of specimen in 0.0025 M in situ synthesized inhibitor is so bright and seems to be etched slightly.

The FTIR reflectance spectrum of corrosion layer formed on the steel surface after immersion in 0.5 M H_2SO_4 with 0.0025 M in situ synthesized inhibitor and the 2-phenyl-1H-benzo[d]imidazole which is synthesized in the laboratory is shown in Fig. 14a. The band at 3428.3 cm^{-1} is attributed to N H stretching and 1625.91 cm^{-1} is for C N stretching. The other peaks are attributed to C H aromatic bands [39]. As it is shown in the molecular struc-

ture of the commercial 2-phenyl-1H-benzo[d]imidazole (Fig. 14b) these kinds of bands are typical for this material. So we can conclude that this organic compound is produced with the in situ manner on the metal surface in 0.5 M H_2SO_4 solution.

In quantum chemical studies we can mention the energy of HOMO that is often associated with the electronic donating ability of a molecule. Therefore, an increase in the values of E_{HOMO} can facilitate the adsorption and therefore the inhibition efficiency, by indicating the disposition of the molecule to donate orbital electrons to an appropriate acceptor with empty molecular orbitals [14,47]. The energy of LUMO on the other hand, indicates the ability of the molecule to accept electrons. The lower the value of E_{LUMO}, the more probable it is that the molecule accepts electrons [14]. In the same way, low values of the energy of the gap $\Delta E = E_{LUMO} - E_{HOMO}$ will render good inhibition efficiencies, because the energy to remove an electron from the last occupied orbital will be low [15]. Increasing values of dipole moment has been reported to facilitate adsorption (and therefore inhibition) by influencing the transport process through the adsorbed layer. So, the inhibition efficiency increases with increasing values of the dipole moments [14]. Table 7 data reveal that although 2-phenyl-1H-benzo[d]imidazole does not get the highest E_{HOMO} and the lowest E_{LUMO}, but it has the smaller energy gap ($\Delta E = E_{LUMO} - E_{HOMO}$) and the greater Dipole moment (μ) as compared to other molecules which indicate the better inhibition efficiency rather than its components.

5. Conclusions

From the present study, the following main conclusions can be drawn:

1. In situ synthesis of the inhibitor has great effect on achieving high efficiencies compared with its components. In fact a new inhibitor with high efficiency obtained from two components which have not inhibitive properties. The beneficial condition among the in situ synthesized inhibitors concentration was 0.0025 M with the approximate efficiency of 97% and it is equal to the efficiency of 2-phenyl-1H-benzo[d]imidazole.
2. In situ synthesized inhibitor acts as an adsorptive inhibitor. It reduces anodic dissolution, retards the hydrogen evolution reaction via blocking the active reaction sites on the metal surface and its adsorption obeys the Langmuir's adsorption isotherm.
3. The results show that by increasing time the R_p of acid decreases while it increases in the case of inhibitor.
4. Evaluating temperature effect on efficiency of in situ synthesized inhibitor at 0.0025 M concentration indicates that corrosion current densities increases with rising temperature, they always are lower than blank solution one.
5. Thermodynamic adsorption parameters such as ΔG°_{ads}, ΔH°_{ads} and ΔS°_{ads} show that the in situ synthesized inhibitor adsorbed by an exothermic process and its adsorption is physical adsorption.
6. Data obtained from weight loss and electrochemical measurements are strongly comparable and have shown that the in situ synthesized inhibitor has the very good inhibiting properties for mild steel in H_2SO_4 solution.
7. Optical microscopy obviously shows the corrosion attack morphology in absence and presence of inhibitors in 0.5 M H_2SO_4 solution and it depicts that mild steel surface severely corrodes if inhibitors are not used.
8. The results obtained from FTIR spectra proved that 2-phenyl-1H-benzo[d]imidazole synthesized on the metal surface from the combination of benzene-1,2-diamine and benzaldehyde along with ferric chloride catalyst in electrolyte solution.
9. Quantum chemical study reveals that the benzene ring and N atoms can be suitable sites for adsorption onto surface. This is pronounced for N atoms because of having lone pair of electrons.

Acknowledgements

Authors would like to appreciate the financial support from Ferdowsi University of Mashhad provision of laboratory facilities during the period that this research was conducted. Corresponding author likes to express her grateful thanks to Mr. Mojtaba Momeni for his encouragement during the preparation of the manuscript.

References

[1] H.H. Uhling, R.W. Revie, Corrosion and Corrosion Control, Wiley, New York, 1985.
[2] V.S. Sastri, Corrosion Inhibitors, Principles and Applications, John Wiley and Sons, New York, 1998.
[3] A. Raman, P. Labine, M.A. Quraishi (Eds.), Reviews on Corrosion Inhibitor Science and Technology, vol. 3, Springer, Berlin, 2004.
[4] N.S. Ayati, S. Khandandel, M. Momeni, M.H. Moayed, A. Davoodi, M. Rahimizadeh, Inhibitive effect of synthesized 2-(3-pyridyl)-3,4-dihydro-4-quinazolinone as a corrosion inhibitor for mild steel in hydrochloric acid, Mater. Chem. Phys. 126 (2011) 873–879.
[5] I. Ahamad, M.A. Quraishi, Bis (benzimidazol-2-yl) disulphide: an efficient water soluble inhibitor for corrosion of mild steel in acid media, Corros. Sci. 51 (2009) 2006–2013.
[6] L. Herrag, B. Hammouti, S. Elkadiri, A. Aouniti, C. Jama, H. Vezin, F. Bentiss, Adsorption properties and inhibition of mild steel corrosion in hydrochloric solution by some newly synthesized diamine derivatives: experimental and theoretical investigations, Corros. Sci. 52 (2010) 3042–3051.
[7] L. Wang, Evaluation of 2-mercaptobenzimidazole as corrosion inhibitor for mild steel in phosphoric acid, Corros. Sci. 43 (2001) 1637–1644.
[8] H. Amar, A. Tounsi, A. Makayssi, A. Derja, J. Benzakour, A. Outzourhit, Corrosion inhibition of Armco iron by 2-mercaptobenzimidazole in sodium chloride 3% media, Corros. Sci. 49 (2007) 2936–2945.
[9] J. Cruz, R. Martínez, J. Genesca, E. García-Ochoa, Experimental and theoretical study of 1-(2-ethylamino)-2-methylimidazoline as an inhibitor of carbon steel corrosion in acid media, Electroanal. Chem. 566 (2004) 111–121.
[10] M.A. Khalifa, M. El-Batouti, F. Mahgoub, A. Bakr Aknish, Corrosion inhibition of steel in crude oil storage tanks, Mater. Corros. 54 (2003) 251–258.
[11] O. Benali, L. Larabi, M. Traisnel, L. Gengembra, Y. Harek, Electrochemical, theoretical and XPS studies of 2-mercapto-1-methylimidazole adsorption on carbon steel in 1M $HClO_4$, Appl. Surf. Sci. 253 (2007) 6130–6139.
[12] F. Bentiss, M. Lebrini, M. Lagrenée, Thermodynamic characterization of metal dissolution and inhibitor adsorption processes in mild steel/2,5-bis(n-thienyl)-1,3,4-thiadiazoles/hydrochloric acid system, Corros. Sci. 47 (2005) 2915–2931.
[13] J. Alijourani, K. Raeissi, M.A. Golozar, Benzimidazole and its derivatives as corrosion inhibitors for mild steel in 1M HCl solution, Corros. Sci. 51 (2009) 1836–1843.
[14] I.B. Obot, N.O. Obi-Egbedi, Theoretical study of benzimidazole and its derivatives and their potential activity as corrosion inhibitors, Corros. Sci. 52 (2010) 198–204.
[15] K.F. Khaled, The inhibition of benzimidazole derivatives on corrosion of iron in 1M HCl solutions, Electrochim. Acta 48 (2003) 2493–2503.
[16] S. Lin, L. Yang, A simple and efficient procedure for the synthesis of benzimidazoles using air as the oxidant, Tetrahedron Lett. 46 (2005) 4315–4319.
[17] H. Eshghi, M. Rahimizadeh, A. Shiri, P. Sedaghat, One-pot synthesis of benzimidazoles and benzothiazoles in the presence of $Fe(HSO_4)_3$ as a new and efficient oxidantbull, Korean Chem. Soc. 33 (2012) 515–518.
[18] G.F. Chen, X.Y. Dong, Facile and selective synthesis of 2-substituted benzimidazoles catalyzed by FeCl3/Al2O3, E-J. Chem. 9 (2012) 289–293.
[19] E. McCafferty, Validation of corrosion rates measured by the Tafel extrapolation method, Corros. Sci. 47 (2005) 3202–3215.
[20] M.A. Amin, M.M. Ibrahim, Corrosion and corrosion control of mild steel in concentrated H_2SO_4 solutions by a newly synthesized glycine derivative, Corros. Sci 53 (2011) 873–885.
[21] A. Kosari, M. Momeni, R. Parvizi, M. Zakeri, M.H. Moayed, A. Davoodi, H. Eshghi, Theoretical and electrochemical assessment of inhibitive behavior of some thiophenol derivatives on mild steel in HCl, Corros. Sci. 53 (2011) 3058–3067.
[22] M.M. Solomon, S.A. Umoren, I.I. Udosoro, A.P. Udoh, Inhibitive and adsorption behaviour of carboxymethyl cellulose on mild steel corrosion in sulphuric acid solution, Corros. Sci. 52 (2010) 1317–1325.
[23] H.H. Hassan, Perchlorate and oxygen reduction during Zn corrosion in a neutral medium, Electrochim. Acta 51 (2006) 5966–5972.

[24] A.K. Singh, M.A. Quraishi, Investigation of adsorption of isoniazid derivatives at mild steel/hydrochloric acid interface. Electrochemical and weight loss methods, Mater. Chem. Phys. 123 (2010) 666–677.
[25] S.A. Ali, H.A. Al-muallem, S.U. Rahman, M.T. Saeed, Bis-isoxazolidines: a new class of corrosion inhibitors of mild steel in acidic media, Corros. Sci. 50 (2008) 3070–3077.
[26] F.S. de Souza, A. Spinelli, Caffeic acid as a green corrosion inhibitor for mild steel, Corros. Sci. 51 (2009) 642–649.
[27] A.Y. Musa, A.A.H. Kadhum, M.S. Takriff, A.R. Daud, S.K. Kamarudin, N. Muhamad, Corrosion inhibitive property of 4-amino-5-phenyl-4H-1,2,4-triazole-3-thiol for mild steel corrosion in 1.0M hydrochloric acid, Corros. Eng. Sci. Technol. 45 (2010) 163–168.
[28] S.M.A. Hosseini, A. Azimi, The inhibition of mild steel corrosion in acidic medium by 1-methyl-3-pyridin-2-yl-thiourea, Corros. Sci. 51 (2009) 728–739.
[29] G. Mu, X. Li, G. Liu, Synergistic inhibition between tween 60 and NaCl on the corrosion of cold rolled steel in 0.5 M sulfuric acid, Corros. Sci. 47 (2005) 1932–1952.
[30] R. Fuchs-Godec, The adsorption, CMC determination and corrosion inhibition of some N-alkyl quaternary ammonium salts on carbon steel surface in 2 M H_2SO_4, Coll. Surf. A Physicochem. Eng. Asp. 280 (2006) 130–139.
[31] G. Avci, Corrosion inhibition of indole-3-acetic acid on mild steel in 0.5 M HCl, Colloid Surf. A 317 (2008) 730–736.
[32] E.A. Noor, A.H. Al-Moubaraki, Thermodynamic study of metal corrosion and inhibitor adsorption processes in mild steel/1-methyl-4[40(-X)-styrylpyridinium iodides/hydrochloric acid systems, Mater. Chem. Phys. 110 (2008) 145–154.
[33] R. Solmaza, G. Kardas, M. Culh, B. Yazici, M. Erbil, Investigation of adsorption and inhibitive effect of 2-mercaptothiazoline on corrosion of mild steel in hydrochloric acid media, Electrochim. Acta 53 (2008) 5941–5952.
[34] R. Solmaz, G. Kardas, B. Yazici, M. Erbil, Adsorption and corrosion inhibitive properties of 2-amino-5-mercapto-1,3,4-thiadiazole on mild steel in hydrochloric acid media, Colloid Surf. A 312 (2008) 1–7.
[35] H. Ashassi-Sorkhabi, B. Shaabani, D. Seifzadeh, Corrosion inhibition of mild steel by some schiff base compounds in hydrochloric acid, Appl. Surf. Sci. 239 (2005) 154–164.
[36] M. Benabdellah, R. Touzani, A. Dafali, M. Hammouti, S. El Kadiri, Mater. Lett. 61 (2007) 1197–1204.
[37] A.Y. Musa, A.A.H. Kadhum, A.B. Mohamad, A.Z. Daud, M.S. Takriff, S.K. Kamarudin, A comparative study of the corrosion inhibition of mild steel in sulphuric acid by 4,4-dimethyloxazolidine-2-thione, Corros. Sci. 51 (2009) 2393–2399.
[38] X. Li, Sh. Deng, H. Fu, G. Mu, N. Zhao, Synergism between rare earth cerium(IV) ion and vanillin on the corrosion of steel in H_2SO_4 solution: Weight loss, electrochemical, UV–vis, FTIR, XPS, and AFM approaches, Appl. Surf. Sci. 254 (2008) 5574–5586.
[39] D. Pavia, G. Lampman, G. Kriz, Introduction to Spectroscopy, Thomson Learning, Washington, 2001.
[40] X. Wang, H. Yang, F. Wang, An investigation of benzimidazole derivative as corrosion inhibitor for mild steel in different concentration HCl solutions, Corros. Sci. 53 (2011) 113–121.
[41] A. Popova, M. Christov, S. Raicheva, E. Sokolova, Adsorption and inhibitive properties of benzimidazole derivatives in acid mild steel corrosion, Corros. Sci. 46 (2004) 1333–1350.
[42] S.A. Umoren, Y. Li, F.H. Wang, Electrochemical study of corrosion inhibition and adsorption behaviour for pure iron by polyacrylamide in H_2SO_4: Synergistic effect of iodide ions, Corros. Sci. 52 (2010) 1777–1786.
[43] E.E. Oguzie, Y. Li, F.H. Wang, Corrosion inhibition and adsorption behavior of methionine on mild steel in sulfuric acid and synergistic effect of iodide ion, Appl. Surf. Sci. 310 (2007) 90–98.
[44] M.K. Pavithra, T.V. Venkatesha, K. Vathsala, K.O. Nayana, Synergistic effect of halide ions on improving corrosion inhibition behaviourof benzisothiozole-3-piperizine hydrochloride on mild steel in 0.5 M H_2SO_4 medium, Corros. Sci. 52 (2010) 3811–3819.
[45] S.S. Abd El Rehim, S.M. Sayyah, M.M. El-Deeb, S.M. Kamal, R.E. Azooz, Poly(o-phenylenediamine) as an inhibitor of mild steel corrosion in HCl solution, Mater. Chem. Phys. 123 (2010) 20–27.
[46] X. Li, S. Deng, H. Fu, G. Mu, Inhibition effect of 6-benzylaminopurine on the corrosion of cold rolled steel in H_2SO_4 solution, Corros. Sci. 51 (2009) 620–634.
[47] Gokhan Gece, The use of quantum chemical methods in corrosion inhibitor studies, Corros. Sci. 50 (2008) 2981–2992.